Origin of the high frequency variability of bio-optical properties in complex coastal environments.

P.R. Renosh[1], H. Loisel[2], F.G. Schmitt[1], X. Meriaux[2], A. Sentchev[2] and G. Lacroix[3]

[1]University of Lille-1Science and Technology,CNRS, Laboratory of Oceanology and Geosciences, UMR 8187 LOG, 32 Avenue Foch, 62930 Wimereux, France.

[2]ULCO, CNRS, Laboratory of Oceanology and Geosciences, UMR 8187 LOG, 32 Avenue Foch, 62930 Wimereux, France.

[3]Remote Sensing and Ecosystem Modelling (REMSEM) teamManagement Unit of the North SeaMathematicalModels(MUMM)Gulledelle100 B-1200 BRUSSELS.

Renosh.Pr@univ-lille1.fr

Abstract

This study describes physical processes (mainly the turbulence and re-suspension of particles due to turbulence) which control the micro scale variability of the bio-optical properties in highly turbid coastal waters. Time series analyses of different bio-optical and physical properties (temperature, salinity) have been performed from a boat in coastal waters. The data base gathers high frequency (1 Hz) simultaneous measurements performed during about 12 hours at four different days and locations in the highly turbid coastal environments of North Sea. We mainly focus on the concentrations of Chlorophyll and coloured detrital matter, back-scattering, and attenuation. For each parameter we consider the statistics (mean values, coefficients of variance and probability density functions) and the dynamics (Fourier power spectra). We found that these optical parameters (b_{bp}, b_p-slope γ, Refractive index-n and c_p) are influenced by turbulence and inherit some of turbulence characteristics; high frequency noise, scales of variability at lower frequencies.

Keywords: Coastal Environments, Bio-Optical Properties, Turbulence.

1. Introduction

The fluctuations in the density field and refractive index of an oceanic fluid are controlled by the turbulent fluctuations, which are well observed through passive scalars such as Temperature, T, and Salinity, S. Almost all oceanic flows are turbulent and are characterised by a wide range of coexisting scales of motion. The turbulence field also affects the spatial and temporal variability of the particulate and dissolved matter. In situ measurements of inherent optical properties (IOPs) as well as of fluorescence properties of phytoplankton and colored dissolved organic matter, performed at relatively high frequency, allow the impact of turbulence on the particulate and dissolved matter pool to be examined. For instance, while particulate backscattering (b_{bp}; m^{-1}) and scattering (b_p, m^{-1}) coefficients both give information on the concentration of particles, their respective ratio (b_{bp}/b_p) is sensitive to the size distribution and refractive index of the bulk particulate matter (Loisel and Morel

1998; Twardovski et al., 2001; Babin et al. 2003; Loisel et al. 2007; Neukermans et al., 2012). Note that, in contrast to the scattering in the backward direction (from 90° to 180°), forward scattering up to 0.1° is dominated by turbulence-induced scattering from inhomogeneities in the refractive index of seawater(Bogucki et al., 1998 and references therein).The spectral shape of the particulate attenuation coefficient, c_p (m^{-1}), may be used as a good proxy of the slope of the particulate size distribution, γ, assuming that the latter follows a Junge-type distribution (Morel, 1976; Boss et al., 2001). In the same way, and after correction of the spectral absorption effect, the spectral slope of b_p can be used to estimate the PSD slope (Doxaran et al., 2009).

In the present paper we discuss the impact of turbulence on the variability of the concentration of particles (trough b_{bp} and b_p), their bulk refractive index (i.e. b_{bp}/b_p) and size distribution (i.e. b_p spectral shape), Chl, CDOM, as well as passive tracers such as T and S.

2. Data and Methods

Four long-time measurements (about 12 hours each) were conducted from January to July 2010 (26-January-2010, 19-April-2010, 21-April-2010 and 07-July-2010) in the coastal waters of Southern North Sea(Fig. 1). The time series of bio-optical properties as well as physical properties (T, S) have been collected from an optical package composed by a CTD (Sea Bird), an ac-s (WET Labs) , c-star (WET Labs), ECO-BB-9 (WET Labs), ECO-FLRT (WET Labs) and ECO-FLCDRT(WET Labs). Every hour, a profile of the water column is performed to assess the vertical structure of the particulate matter, and especially the re-suspension effects. The examinations of the vertical patterns are out of the scope of the present study.

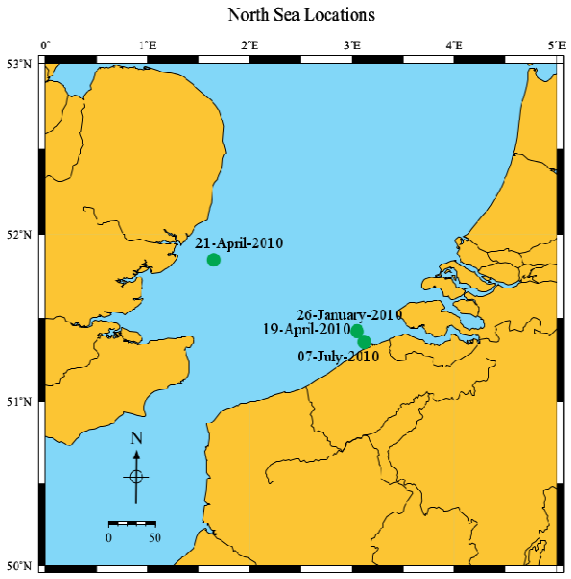

Fig. 1. Study area: South of North Sea

The ac-s measures the absorption and attenuation spectra with a 4 nm spectral resolution between 400 to 730 nm with 15 nm band widths, has a 10-cm path length and an in-water acceptance

angle of 0.93°. A MilliQ water calibration were carried before and after of each field campaigns. The scattering coefficient is extracted from the ac-s instruments because the pre and post calibration of ac-s with MilliQ water the spectral difference between attenuation and absorption directly gives the particulate scattering coefficient (b_p). The c-star measures c at 660 nm (+/- 20 nm) over a 10 cm path length and has an in water acceptance angle of 1.2°. The c-star instrument was calibrated by WET labs on a yearly basis and additional calibrations with MilliQ water were carried out three times per campaign. After calibration, c-star measurement directly gives c_p (m^{-1}), assuming that coloured dissolved organic matter does not absorb at 660 nm. The Salinity, Temperature and Depth were measured from the CTD instrument (Seabird). The backscattering coefficients at nominal wavelengths of 488, 510, 532, 595, 650, 676, 715, 765 and 865 nm were collected with the ECO-BB-9. It records the volume scattering function, β at a fixed angle in the backward direction (124°). The data conversion from raw β to calibrated β was performed using the WAP software provided by WETlabs. Data were corrected for temperature and absorption effects, and the scattering contribution by pure sea water to β was subtracted to obtain particulate volume scattering function βp following Zhang et al. (2009). Particulate backscattering coefficients, b_{bp}, were obtained from βp by multiplying by $2\pi\chi$, with χ = 1.1(Sullivan and Twardowski 2009). The ECO-BB-9 was calibrated by WETLabs on a yearly basis. An additional correction of b_{bp} by a factor 0.82 (= 0.9:1.1) was applied following Sullivan et al. (2005).

Hyperbolic slope of b_p is computed for the entire cruises using the wavelength range from 555 nm to 741 nm using (the blue part of the spectrum is not taken into account to limit the depressing effects due to absorption):

$$b_p(\lambda) \approx b_p(\lambda_0)\left(\frac{\lambda_0}{\lambda}\right)^{\gamma} \quad (1)$$

where λ_0 is the reference wavelength.Bulk refractive Index (n) is computed using (Twardowski et al., 2001):

$$n = 1 + a\left(\frac{b_{bp}}{b_p}\right)^{z} \quad (2)$$

where a = 1.671, z = 0.582 (Twardowski et al., 2001). In the following the value of n is estimated using equation(2), knowing b_{bp} and $b_p$from the measurements.

3.Temporal series visualisation

An example of the temporal series of the different parameters measured the 21 of April 2012 are presented in Figure 2. The intrusion of coastal water masses is clearly seen at the beginning of the night period the 21 of April, with a sharp increase of S (and an decrease of T). While Chl, C_p, and b_{bp} present the same temporal evolution, CDOM presents a different pattern, with a decrease trend during day time, and an increase when the salinity changes. These water masses are characterized by a decrease of CDOM value corresponding increase in the salinity. From the figure 2E and 2G there is a good agreement of C_p and b_{bp} data in the temporal scale. This is observed in all the four days.There is an inverse agreement seen the Refractive Index and b_p-slope (ɣ) in the temporal scale.

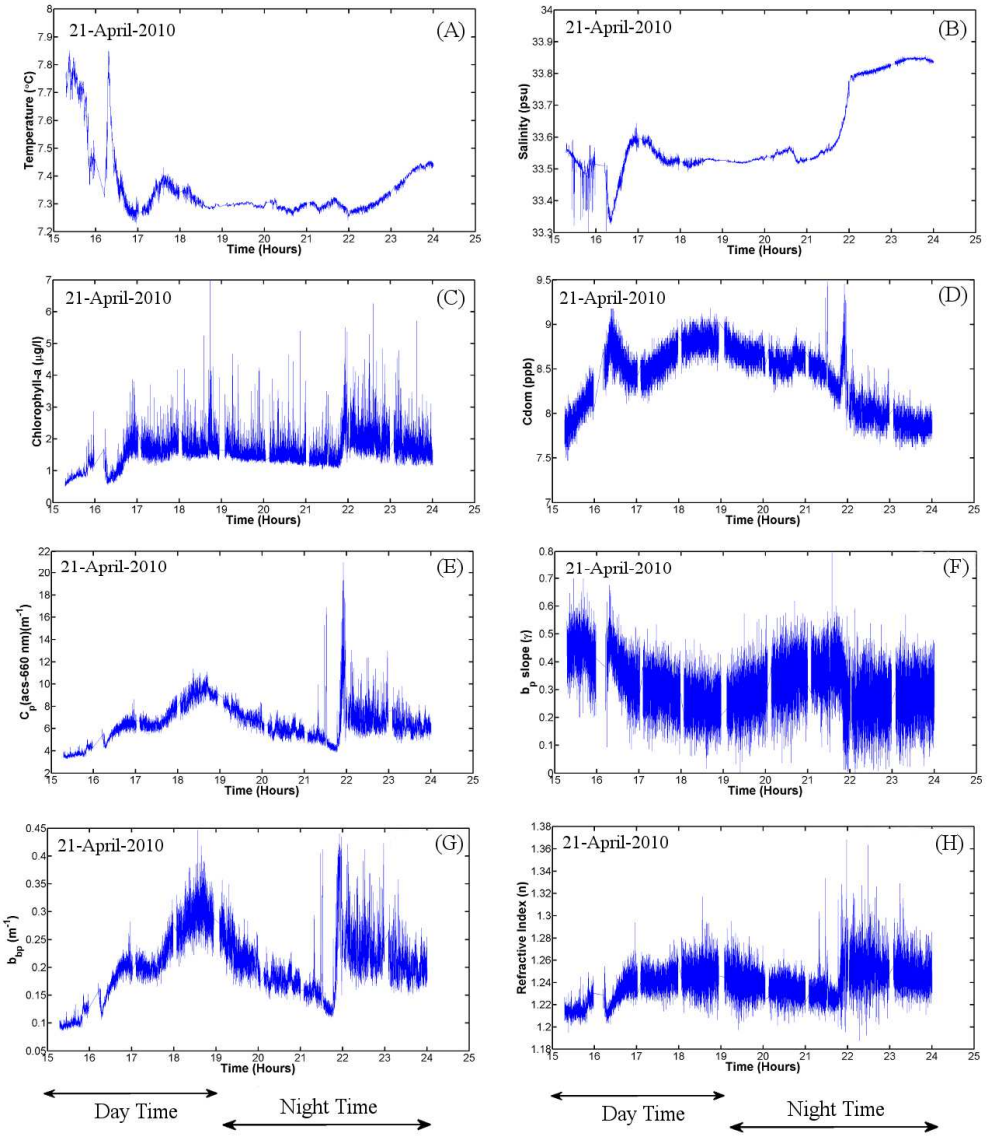

Fig. 2. Time series observation of different parameters: Temperature, Salinity, Chlorophyll-a, CDOM, C_p-660 nm, b_p slope(γ),b_{bp}-532 nm and Bulk refractive Index(n) of day 21-April-2010

4. Comparison of mean and coefficient of variance

The mean and coefficient of variation (standard deviation divided by the mean) values of the different measured parameters are given in Table 1 with the mean physical parameters modelled using a regional coupled physical-biogeochemical model (Lacroix et al., 2007). The Chl and SPM values are those measured in situ at some given time periods during the continuous measurements.The integrated current velocities for the four experiments are about the same (around 9 m^2s^{-1}), except at the station visited the 19 of April when it is two times greater, due to deeper bottom depth at this

station. While the mean chlorophyll concentration varies between 1 and 3 mg.m^{-3} for three stations, its values increases by about a factor of 10 the 19 of April. This station is dominated by a phytoplankton blooms (*Phaeocystisglobosa*). The minimum mean CDOM value is observed the 21 of April (the more offshore station) while the three others stations exhibits about the same mean value.

Stations	Station Depth(m)	Statistics	Chl-a mg.m^{-3}	SPM (mgL^{-1})	Res. Wind (m/s)	Res. Dep. Int. Vel. (m²/s)	B. Stress (m²/s²)	Chl-a Flo (µg/l)	Cdom Flo (ppm)	c_p- cstar 660 nm (m^{-1})	c_p- ac-s 660 nm (m^{-1})	b_{bp}-532 (m^{-1})	b_p-532 (m^{-1})	b_{bp}/b_p (532 nm)	Temperature (°C)	Salinity (psu)	b_p-slope (γ)	Refractive Index
26-01-2010	16.75	N	11	13	48	48	48	32627	32627	32627	32627	12412	12412	12412	32627	32627	32128	12412
		Mean	0.54	35.41	5.20	9.82	0.0008	0.99	15.20	11.72	17.22	0.212	8.281	0.026	3.15	31.98	0.471	1.198
		Coef. V.	34.82	64.08	17.99	34.83	52.64	30.99	4.81	46.64	53.59	11.46	10.86	4.69	3.59	0.55	20.29	0.43
19-04-2010	16.75	N	9	12	48	48	48	28826	28826	28826	28826	15651	15651	15651	28826	28826	28826	12412
		Mean	15.44	14.23	3.88	8.73	0.0006	33.55	12.94	5.73	5.57	0.078	3.505	0.021	8.74	31.33	0.242	1.178
		Coef. V.	28.79	66.82	20.24	32.14	47.83	29.21	5.55	31.72	50.71	51.470	32.640	17.290	2.27	1.01	82.90	1.500
21-04-2010	29.75	N	11	12	48	48	48	28170	28170	28170	28170	27943	27943	27943	28170	28170	28147	12412
		Mean	2.58	9.42	2.79	19.51	0.0010	1.56	8.41	4.01	6.53	0.204	6.656	0.036	7.35	33.60	0.313	1.240
		Coef. V.	48.94	53.75	19.91	46.92	65.43	27.80	4.13	17.01	25.62	27.600	18.870	10.960	1.59	0.39	29.18	1.210
07-07-2010	13.75	N	3	3	48	48	48	46269	46269	46269	46269	32377	32377	32377	46269	46269	46245	12412
		Mean	2.27	3.74	3.25	7.27	0.0006	3.24	13.03	5.82	7.68	0.184	7.073	0.026	19.44	29.77	0.398	1.198
		Coef. V.	30.99	122.58	28.91	43.12	63.18	16.13	5.32	33.29	38.17	42.300	37.780	11.720	0.51	0.37	25.98	1.100

Table 1: Mean and coefficient of variations of different parameters. SPM and Chl-a are measured from water samples taken at different time of the experiments.

The highest value of scattering coefficient is observed in the station sampled on 26 of January and the percentage variance in scattering coefficient in this station is low. This station shows around 11% of variancein scattering coefficient;this variance is less compared to other three stations. From the SPM and Chl values it shows that this high b_p value in the scattering coefficient is mainly due to the high concentration of sediment load in this station, the mean values of SPM is around 35 mg.L^{-1}, this value is very high compared to other stations. The low value in the scattering coefficient is observed at the station sampled on the 19 of April even though it is still comparatively high concentration of SPM. The reduction of the scattering coefficient value in this station is mainly due to the masking of scattering coefficient due to high absorption of phytoplankton due to phytoplankton bloom. The other 2 stations show a high mean value compared to the 19 of April.

Coming to the backscattering coefficient we can see that there is a relatively low value similar to like scattering coefficient in the station sampled in 19 of April. This mean value of backscattering coefficient at this station is 0.078 m^{-1}, while the other stations are characterized by a b_{bp} value which is about 2.5 times greater. The presence of relatively large phytoplankton particles with lower refractive index compared to smaller ones at this station may explain this difference.

The difference in the rough characteristics of the bulk particulate matter assembles between stations can be assessed by looking at the b_p spectral slope and the b_{bp}/b_p values. While the mean slope value of the particulate size distribution is about the same during the different experiments, the average chemical nature of the bulk particulate matter slightly differs. The b_{bp}/b_p ratio for all the sampling dates varies between 0.02 to 0.036 with a coefficient of variation between 4.5 to 17.3 %.

The Chl-fluorescence signal exhibits a much higher coefficient of variation than the CDOM-fluorescence signal, mainly due to the complex phytoplankton assemblage characterized by different fluorescence quantum yield, as well as by difference in the photosynthetic available radiations between stations (depending on the season, cloud cover, turbidity, etc). While, for a given stations, the chemical nature of the bulk particulate matter does not change drastically over the recorder time, the particulate size distribution slope (still assuming a hyperbolic shape) exhibits much greater variability (between 20 to 80%).

5. Probability density function estimates of n and γ

Here we show a more complete view of the variability of the refractive index (n) and the b_p-slope (γ), by estimating their probability density functions (pdf), shown in Fig. 3 and 4.

The refractive index is estimated at each time step using Eq. (2). Fig. 3 shows that it has a range of values depending on the sampling day. In all cases the mean values are similar (around 1.2) and the coefficient of variations are small (between 0.4 and 1.5); the pdf can confirm this and show that the variability of n is in general asymmetric, especially on 19 April 2010.

The b_p-slope (γ) estimates are shown in Fig. 4; Table 1 showed that the mean values are somewhat different (between 0.24 and 0.47) with quite high variability (coefficient of variation between 10% and 82%), but the shapes of their pdf also give interesting results:

- On 26-January the pdf is bimodal, with two modes (0.35 and 0.55)
- On 19-April (bloom station) there is a symmetric unimodal shape with high dispersion.
- On 21-April it is also unimodal, but with a narrower shape (mode at 0.3)
- On 07-July it is unimodal with a non-symmetric distribution and a mode of 0.45.

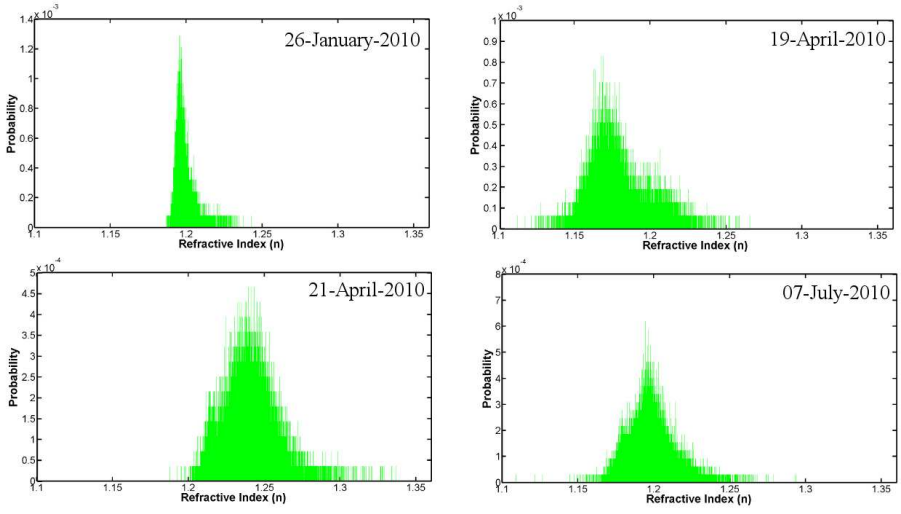

Fig. 3. Probability Density Function of Refractive Index (n) for all the 4 days. The same horizontal scale is used for comparison.

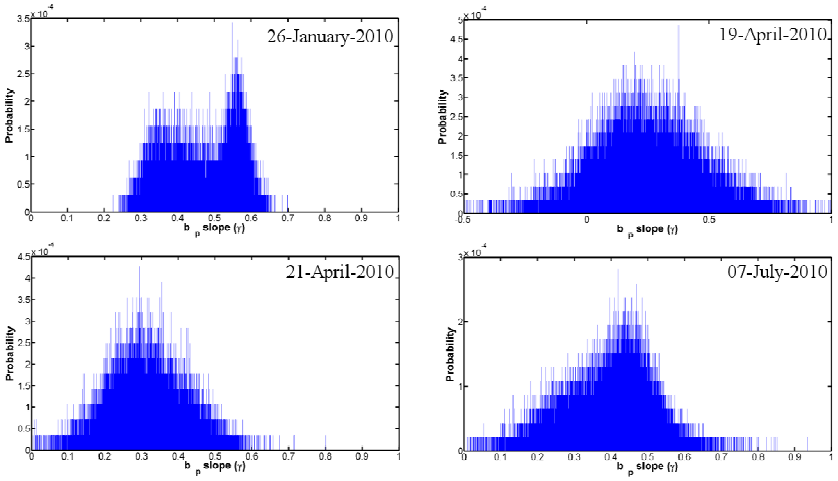

Fig. 4. Probability Density Function of b_p-slope (γ) for all the 4 days.

6. Dynamics of the parameters and relation with turbulence

Here we estimate the Fourier power spectra in log-log plots, in order to have information on the stochastic dynamics of the series and their relation with turbulence. Since there are gaps in the series, we estimates the Fourier power spectra by computing first the auto correlation function C(τ) and estimates the energy E(f) as (Fourier Khinchien theorem):

$$E(f) = \frac{1}{2\pi}\int_0^{\infty} \cos(2\pi ft) C(t)\, dt \qquad (3)$$

Fig 5 shows the energy spectra of several parameters, for 21 April 2010; for display reason we cannot show all the series; the 21 April results are here shown as example and representative of other days.

- Fig. 5Ashows the power spectra of T and S series. These are turbulent passive scalars (Monin and Yaglom 1975). In 3D locally homogeneous turbulence they have typically a 5/3 spectrum (Kolmogorov-Obukhov-Corrsin law) thus a power law with slope -5/3 is shown in the plots for comparison. We see that such power law is quite well respected at lower frequencies (> 0.05 S^{-1}) there are horizontal lines corresponding to noise; it could be due to the sensor(instrument noise) or the measurement quantities themselves (not likely). In the following we take this -5/3 range as a turbulence indicator.
- Fig. 5B shows the power spectra for Chl and CDOM. These quantities show the same typical behaviour; power law slopes for lower frequencies and noise for high frequencies. Chla seems here to be advected by turbulence, like a passive scalar (Seuront et al., 1996). The CDOM time series is behaving the same way and here estimated for the first time.
- Fig. 5C-Eshows the power spectra for other optical parameters. These parameters have some variability, but have never been studied this way be focussing on their dynamics. Here we see that they have a turbulent like stochastic behaviour similar with passive scalars but with

some difference due to the fact that they are estimated using nonlinear transformations.They show some high frequency noise but they are not noisy for all frequencies and they do show some power law decrease indicating correlation in the series; however it could be that a different slope (smaller than 5/3) could be a better power law fit in some cases.

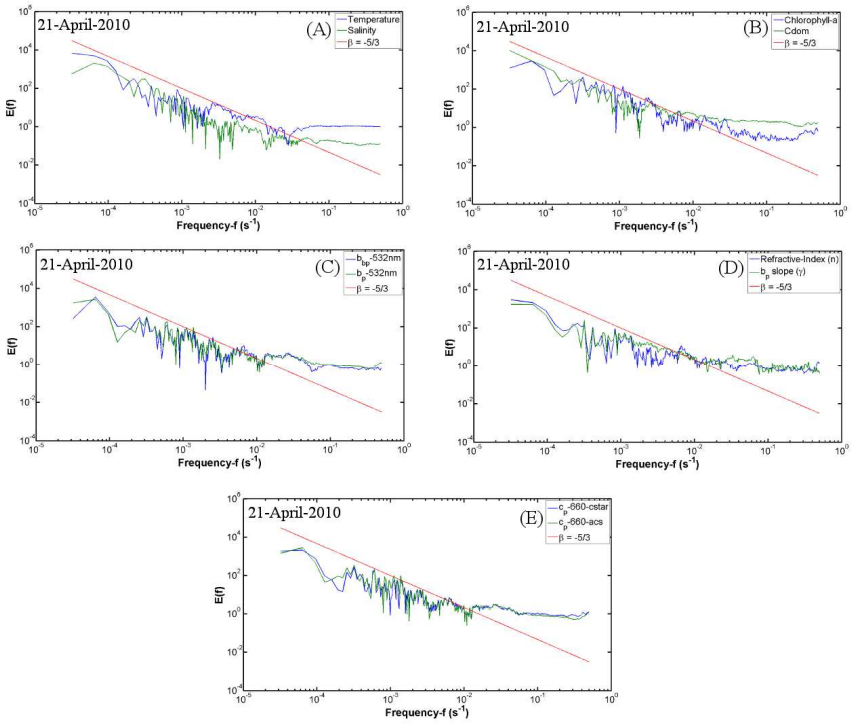

Fig. 5. Power spectra of different parameters observed on 21-April-2010

Conclusions

In this preliminary study, we estimated simultaneous turbulence (S,T) and optical parameters at high frequency and considered their stabilities (mean, coefficient of variance and pdf) and their dynamics using power spectra. We found that these optical parameters (b_{bp},b_p-slope (ɣ),Refractive index-n and c_p) are influenced by turbulence and inherit some of turbulence characteristics; high frequency noise, scales of variability at lower frequencies. Future experiments will encompasses in situ particle size measurements, as well as field turbulence measurements.

Acknowledgments

This first author was supported by the Centre National d'EtudesSpatiales (CNES), and the Centre National de la RechercheScientifique (CNRS) in the frame of a PhD funding. The crews of research vesselBelgicaare thanked for their kind help during sea campaigns. This work has been founded by CNES in the frame of the TOSCA/COULCOT project. Special thanks to Kevin Ruddick who invited us on the Belgica in the frame of the Belcolour-2 project.

References

Antoine, D., Siegel, D. A., Kostadinov, T., Maritorena, S., Nelson, N. B., Gentili, B., Vellucci, V., and Guillocheau, N., Variability in optical particle backscattering in contrasting bio-physical oceanic regimes, *Limnol. Oceanogr*., 56, 955-973, 2011.

Babin,M., Morel, A., Fournier-Sicre, V., Fell, F., and Stramski, D., Light Scattering properties of marine particles in the coastal and oceanic waters as related to the particle mass concentration. *Limnol.Oceanogr*. 48, 843-859, 2003.

Bogucki, D., J. A. Domaradzki, D. Stramski, and J. R. V. Zaneveld, Comparison of near-forward light scattering on oceanic turbulence and particles. *Appl. Opt.*, 37, 4669-4677, 1998.

Boss, E., M. S. Twardowski, and HerringS., The shape of the particulate beam attenuation spectrum and its relation to the size distribution of oceanic particles, *Appl. Opt*.40, 4885– 4893, 2001.

Doxaran D., Ruddick K. McKee D., Gentili B., Tailliez D., Chami M., and Babin. M.,Spectral variations of light scattering by marine particles in coastal waters, from the visible to the near infrared. *Limnol. Oceanogr*. 54, 1257-1271, 2009.

Lacroix, G., Ruddick, K., Park, Y., Gypens, N., Lancelot, C., Validation of the 3D biogeochemical model MIRO&CO with field nutrient and phytoplankton data and MERIS-derived surface chlorophyll a images. *J. Mar. Syst*. 64(1-4), 66-88,2007.

Loisel, H. and Morel, A. Light scattering and chlorophyll concentration in case 1 waters: a re-examination, *Limnol. Oceanogr*. 43, 847-857,1998.

Loisel, H., Meriaux, X., Berthon, J.F., and Poteau, A., Investigation of the optical backscattering to scattering ratio of marine particles in relation to their biogeochemical composition in the eastern English channel and southern North Sea, *Limnol.Oceanogr*. 52, 739-752, 2007.

Monin, A. S. and A.M. Yanglom, *Statistical fluid mechanics: mechanics of turbulence*, MIT Press, Cambridge, 1975.

Morel, A., *Diffusion de la lumière par les eaux de mer; résultats expérimentaux et approche théorique,* AGARD Lect. Ser., 3.1.1–3.1.76, 1976.

Neukermans, G., Loisel, H., Mariaux, X., Astoreca, R., and Mckee, D., In situ variability of mass specific beam attenuation and backscattering of marine particles with respect to particle size, density and composition. *Limmol.Oceanogr*.57(1), 124-144, 2012.

Seuront. L., Schmitt. F., Lagadeuc. Y., Schertzer. D., and Lovejoy. S., Multifractal analysis of phytoplankton biomass and temperature in the ocean. *Geophys. Res. Lett*.23, 3591-3594, 1996.

Stramski, D., Boss,E., Bogucki, D., and Voss, K. J., The role of seawater constituents in light backscattering in the ocean, *Prog. Oceanogr*. 61, 27-56,2004.

Sullivan, J. M., and Twardowski, M. S., Donaghay, P. L., and Freeman, S. A., Use of optical scattering to discriminate particle types in coastal waters. *Appl. Opt*. 44, 1667-1680, 2005.

Sullivan, J. M., and Twardowski, M. S.: Angular shape of the oceanic particulate volume scattering function in the backward direction. *Appl. Opt*. 48, 6811-6819, 2009.

Twardowski, M. S., Boss, E., Macdonald, J. B., Pegau, W.S., Bernard, A. H., and Zaneveld, J. R. V., A model for estimating bulk refractive index from the optical backscattering ratio and the implications for understanding particle composition in case l and case ll waters, *J. Geophys. Res*. 106, 14129-14142, 2001.

Zhang, X. D., Hu, L. B., Twardowski, M. S., and Sullivan. J. M., Scattering by solutions of major sea salts. *Opt. Express* 17, 19580-19585, 2009.